

History Dependence of Rate Covariation between Neurons during Persistent Activity in an Oculomotor Integrator

Emre Aksay^{1*}, Guy Major^{1*}, Mark S. Goldman^{2,3}, Robert Baker⁴, H. Sebastian Seung² and David W. Tank¹

¹Departments of Molecular Biology and Physics, Princeton University, Princeton, NJ 08544, USA, ²Howard Hughes Medical Institute, Brain and Cognitive Sciences Department, MIT, Cambridge, MA 02139, USA and ⁴Department of Physiology and Neuroscience, NYU Medical Center, New York, NY 10016, USA

³Present address: Department of Physics, Wellesley College, Wellesley, MA 02481, USA

*These authors contributed equally.

Persistent firing in response to a brief stimulus is a neural correlate of short-term memory in a variety of systems. In the oculomotor neural integrator, persistent firing that encodes eye position is maintained in response to transient saccadic eye-velocity commands. To a first approximation, firing rates in the integrator vary linearly with eye position. Thus, viewed across many cells, the pattern of persistent firing in the integrator may be constrained to a unique line of stable states. Here this idea was tested by examining the relationship between firing rates of simultaneously recorded neurons. Paired recordings were obtained in awake goldfish from neurons in hind-brain area I, an essential part of the horizontal eye-position integrator. During spontaneous eye movements consisting of sequential fixations at different horizontal positions, the pair relationship between the majority of cells on the same side of the integrator was not unique: for a given rate of one cell, the rate of the paired cell assumed different values that depended systematically on the preceding saccade history. This finding suggests that the set of persistent firing states that encode eye position is not constrained to a unique line, and that models with stable states restricted to a such a line need to be modified accordingly.

Introduction

Sustained discharge elicited by a brief stimulus, or persistent neural activity, is often directly related to information held in short-term memory (reviewed in Durstewitz *et al.*, 2000; Wang, 2001). Persistent activity in cortex has been found to be correlated with memory of visual (Fuster and Alexander, 1971; Funahashi *et al.*, 1989; Gnadt and Anderson, 1988), auditory (Nakamura, 1999; Romanski and Goldman-Rakic, 2002) and tactile (Romo *et al.*, 1999) stimulation. In some experiments, the variable to be memorized can assume a range of values, and these values are encoded by varying persistent rates of firing. In the case of vibrotactile stimuli, the rate of persistent activity changes monotonically with remembered stimulus frequency (Romo *et al.*, 1999; Brody *et al.*, 2003). Monotonic, or graded, short-term memory has an analogy in a well-studied oculomotor system controlling eye position.

In the oculomotor neural integrator, to a first approximation, the discharge of neurons showing persistent activity encodes the time integral of saccadic eye-velocity commands. This ensemble activity is, in effect, an internal memory of eye position. This activity is illustrated schematically in Figure 1. As the eyes step through a series of saccades and fixations, firing rates of pre-motor eye-position-encoding neurons first burst or pause at saccade initiation and then show a step-like sustained rate that increases with the temporal eccentricity of the eye (Fig. 1a). Each 'position' neuron's response can be described by a threshold linear relationship between eye position and firing

rate, with different neurons having different slopes and thresholds (Fig. 1b). This reproduces the qualitative trend of electrophysiological data recorded from position-encoding pre-motor neurons (Luschei and Fuchs, 1972; King *et al.*, 1981; Lopez-Barneo *et al.*, 1982; Delgado-Garcia *et al.*, 1989; Fukushima *et al.*, 1990; McFarland and Fuchs, 1992; Pastor *et al.*, 1994; Aksay *et al.*, 2000).

In both the vibrotactile and oculomotor examples of graded short-term memory, the close coupling between the activity of individual cells and the memory parameter suggests there is a constrained relationship between the persistent rates of the neurons. In the oculomotor example, if persistent activity is exactly linearly correlated with eye position, then, when the firing rate of one neuron is plotted against the firing rate of a second, the relationship would also be represented by a straight line (Fig. 1c). Each point along the line would correspond to a separate unique position of eye fixation. The internal representation of eye position would then be parametrically encoded by distance along the line. Random noise in the system may lead to some scatter about a line of the fixation points, but no systematic variation of the basic structure.

Such tight constraint of the pattern of stable states that can be used to encode memory may yield clues about the underlying mechanism of persistent activity. Some recurrent network models of the oculomotor neural integrator are able to generate patterns of persistent activity like the relationships shown in Figure 1c (Seung, 1996; Seung *et al.*, 2000; Sklavos and Moschovakis, 2002). In some of these studies (Seung, 1996; Seung *et al.*, 2000), it was observed that after transient input forces the network firing pattern off the line, the pattern converges rapidly back to the line; thus, the system behaves as a 'line attractor', with one dimension, or mode, of integration. Other recurrent network models of the integrator have begun exploring multiple modes of integration with the aim of improving robustness with respect to certain perturbations (Cannon *et al.*, 1983; Cannon and Robinson, 1985). Although not explicitly explored by the authors, transient input pushing the network off the line may find new stable states of activity in these models. Another set of models tackle robustness of the network by adding slow dynamics to individual cells or local clusters of cells (Rosen, 1972; Shen, 1989; Koulakov *et al.*, 2002; Goldman *et al.*, 2003). These models can also have less constrained patterns of persistent firing than a one-dimensional configuration of persistent states.

Although conveying the general trend in experimental data, the unique relationship between firing rate and eye position shown schematically in Figure 1b is only an approximation. Recent single-unit studies in area I of the goldfish, a key com-

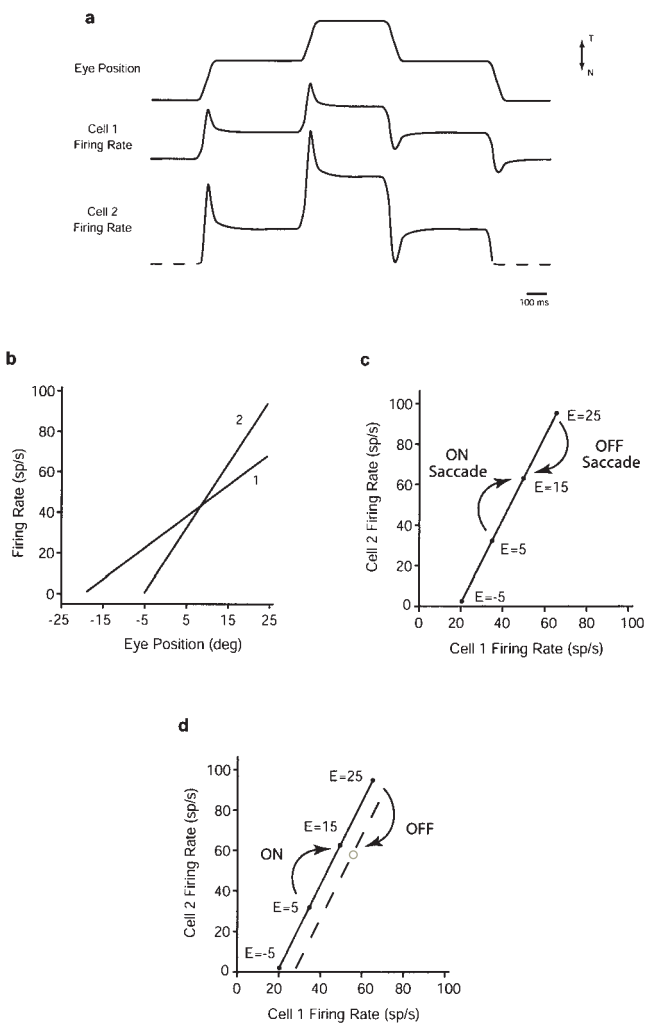


Figure 1. Schematic relationships between rates and eye position in the oculomotor neural integrator inferred from single unit recordings. (a) Position of ipsilateral eye and firing rates of two position cells as a function of time during a sequence of saccades and fixations. T = temporal, N = nasal direction. Dashed line indicates that firing rate is below threshold. (b) Threshold linear relationship of the mean firing rate during fixation versus mean eye position for the two cells in (a). The cells have different slopes and thresholds. (c) Expected relationship between the firing rate of one cell versus the firing rate of the second cell during fixations; the data fall along a single line, regardless of the direction of the preceding saccade. (d) If hysteresis is present in the integrator, the relationship between rates might not be described by a single line. For example, data following off fixations (gray) may fall along a second line (dashed).

ponent of the oculomotor integrator in this species (Aksay *et al.*, 2000), show that the relationship between firing rate and eye position is generally not unique for a given position cell. In fact, one eye position systematically corresponded to two distinct firing rates, depending on the direction from which the eyes arrived. This saccadic history dependence of the firing rate versus eye position relationship has been termed ‘rate-eye hysteresis’. Hysteresis had been previously reported for neurons of the abducens nucleus of primate (Eckmiller, 1974; Goldstein and Robinson, 1986), cat (Delgado-Garcia *et al.*, 1986a,b), rabbit (Stahl and Simpson, 1995a), and goldfish (Pastor *et al.*, 1991),

and for neurons of vestibular nuclei of rabbit that display eye position sensitivity (Stahl and Simpson, 1995b).

Rate-eye hysteresis may indicate a systematic lack of uniqueness in the relationship between the firing rates of different position neurons. In the line attractor conception illustrated in Figure 1c, a unique point on the single line representing eye position can be reached following a saccade from a more nasal or from a more temporal position. However, if the directional asymmetry evident in rate-eye plots originates in the neural integrator, then there may be a non-unique relationship between firing rates. The firing rate versus firing rate relationship of pairs of neurons may depend on the direction of the previous saccade (Fig. 1d). To examine this possibility, we simultaneously recorded pairs of position neurons in area I. These experiments show that, for most pairs, the firing rate-firing rate relationship during steady fixations changes systematically with saccade history. In the following, we term this history dependence of the rate-rate relationships ‘pair hysteresis’.

Materials and Methods

Preparation and Electrophysiology

All experiments were performed in compliance with the Guide for the Care and Use of Laboratory Animals (<http://www.nap.edu/readingroom/books/labrats/>). Specific protocols were approved by the Institutional Animal Care and Use Committee. Goldfish (*Carassius auratus*, 3–5” tip to peduncle, 25–50 g) were purchased from a commercial supplier (Hunting Creek Fisheries, Thurmont, MD) and kept at 18–22°C in large (>50 gallon) aquaria with daily exposure to light. Extracellular recordings were performed on head-restrained awake goldfish with respiratory movements minimized by recirculation of aerated tank water through an oral tube. The methods used for head restraint, surgical preparation, recording of action potentials from single units, spike detection, area I mapping, and eye movement measurements were as described previously (Aksay *et al.*, 2000). The experiments reported here represent recordings from 22 neuron pairs in 14 goldfish. Pairs of neurons were recorded for between 6 and 150 min (median = 68 min).

Data Analysis

Saccade Detection

Saccades were identified in a manner similar to that detailed previously (Aksay *et al.*, 2000), employing an eye velocity or acceleration threshold. For rate-rate scatter plot analysis (Figs 4 and 5), the end of a saccade was identified as the last point exceeding a velocity threshold. For eye-rate scatter plots (Fig. 2) and rate-rate trajectory analysis (Figs 7 and 9), the beginning and end of a saccade were identified as the first and last time points at which the absolute value of acceleration exceeded a threshold. In the following, we refer to the ON direction as nasal-to-temporal movement of the eye ipsilateral to the recorded cell(s), and the OFF direction as temporal-to-nasal movement. An ON fixation is one following an ON saccade.

Mean Firing Rate Calculation in Scatter Plots

Average firing rate was calculated over a window in each fixation. This fixation window began a time t_{aft} after the end of a saccade and ended t_{bef} before the subsequent saccade; if the resulting window was less than a time t_{min} , the fixation was excluded from the subsequent analysis. For the data in Figures 4 and 5, $t_{\text{aft}} = 0.25$ s, $t_{\text{bef}} = 0.25$ s, and $t_{\text{min}} = 0.6$ s; if three or more action potentials occurred within a window, then the firing rate was calculated as the inverse of the mean inter-spike interval. Fixations with fewer than three spikes were not analyzed.

For the data in Figure 2, $t_{\text{aft}} = 0.2$ s, $t_{\text{bef}} = 0.1$ s, and $t_{\text{min}} = 0.5$ s, if three or more action potentials occurred within an initial time period beginning at t_{aft} after the end of the saccade and ending t_{min} later, then the firing rate was calculated as the inverse of the mean inter-spike interval over this period. For this figure, initial periods containing fewer than

three spikes were analyzed with a modified procedure in order to explore very low firing rates. The initial period was extended in 100 ms increments towards, but not beyond, t_{bef} before the start of the next saccade, or until the period contained at least three spikes, whichever came first. Then if there were two or more spikes, inverse mean inter-spike interval over the period was used for rate calculation; however, if there was only one spike, firing rate was calculated as the inverse of this extended initial period.

Firing Rate as a Function of Time

For Figure 3, firing rate functions were calculated as described previously (Aksay *et al.*, 2000), using a sliding rectangular filter window of 150 ms length. For Figures 6–9, in order better to display the underlying slow trends in firing rates during fixations, an alternative method was used which was intended to achieve stronger smoothing of data from as much of each fixation as possible (details in Supplementary material). Spike times were first regularized by a process similar to a ‘mutual repulsion’ algorithm. Next, first the inter-spike intervals and then firing rates were iteratively smoothed with Gaussian filters of decreasing widths, with heavier cumulative smoothing near the middles of fixations and progressively less nearer the edges. The results of each step of this procedure were checked by eye for a large sub-sample of the data against the unprocessed inverse inter-spike intervals, and in all cases satisfactory smoothing was achieved without distortion of the observed underlying trend in firing rate (Fig. 6a).

Trajectory Plots

For the trajectory plots in Figures 7 and 9, the smoothed firing rate of the cell with the lower eye position threshold was plotted on the abscissa, and that of the higher threshold cell was plotted on the ordinate, using a sample interval of 24 ms. Data were used from the first spike at least 500 ms after the end point of a saccade up until the last spike preceding the start point of the next saccade by at least 200 ms. In Figure 7, trajectories during fixations following an ON direction saccade are plotted in black, and those following an OFF direction saccade in gray. Data were excluded within 1 s of ‘blinks’, during fixations following disconjugate saccades, and during episodes of respiratory movements. Rates below 2 spikes/s also were excluded.

Pair Hysteresis Scores

Rate–rate scatter plot scores. For assessment of pair hysteresis in rate–rate scatter plots, the first 20 min segment of data was used that yielded greater than six fixation data points in each group, both ON and OFF. If the total length of data available for a pair was less than 20 min, the entire data set was used. Fifteen of 19 pairs analyzed met the criterion of six points per group. Scores were calculated using the procedure described in the Results section.

Rate–rate trajectory plot scores. For assessment of pair hysteresis in rate–rate trajectory plots, two minimum absolute deviation (‘MAD’) fit lines, one minimizing vertical residuals and the other minimizing horizontal residuals, were obtained for the combined ON–OFF data in each plot, using an algorithm adapted from (Press *et al.*, 1992; www.nr.com). The mean absolute deviation of the residuals from each line was normalized by the 90th percentile of the data along the axis of minimization (including any unplotted points with rates below 2 spikes/s), to obtain a scaled goodness of fit score. The line with the lowest goodness of fit was selected to be the axis about which to compute hysteresis scores (see figure in Supplementary Material for an example). All MAD fit lines were checked by eye and were generally superior to the results of standard least squares linear regression, which tended to give poor fits for vertically oriented data or data with outliers.

The degree of hysteresis was quantified by computing the difference between deviations of the ON trajectories and the OFF trajectories from the MAD line. A perpendicular overlap zone between ON and OFF trajectories was defined as the data between the minimum projection onto the MAD fit line of rates during ON trajectories and the maximum projection onto the line of rates during OFF trajectories (indicated by outermost dashed lines in the supplementary figure). This zone was divided into thin strips perpendicular to the MAD fit line (each pair of dashed lines in the supplementary figure spans 10 strips). Each strip was 1 spikes/s wide when rotated perpendicular to the abscissa. The number

of ON points in the i th strip was designated M_i and the number of OFF points N_i . The pair hysteresis H_i of the i th strip was defined as the median perpendicular distance from the MAD fit line of ON points in the strip minus the median perpendicular distance of OFF points in the strip. The overall perpendicular hysteresis score was calculated as the weighted mean $\Sigma W_i H_i / \Sigma W_i$, with a geometric mean weighting factor $W_i = \sqrt{M_i N_i}$. This score was independent of the intercept of the MAD fit line, and was robust with respect to small changes in the slope.

Scores were calculated for consecutive epochs of time, each epoch between 120 s and 600 s, depending on how much data had been collected for a given pair. At least three epochs with at least one overlapping OFF and ON trajectory were found for all pairs. If the mean perpendicular hysteresis score was significantly different from zero (t -test, $P < 0.05$), the pair was categorized as hysteretic. The perpendicular measure was used because a wide band of trajectories can generate apparent vertical and horizontal hysteresis simply because ON fixations tend to be associated with higher rates than OFF fixations. A percentage perpendicular hysteresis score was then calculated as $80 \times$ mean perpendicular hysteresis score/median 10th–90th percentile range of all ON and OFF points, including rates below 2 spikes/s, projected onto the MAD fit line). This score quantifies the degree of pair hysteresis perpendicular to the MAD fit line as a fraction of the dynamic range of firing rates along the line (both measures depending on both cells). In other words, it is a measure of the separation of the ON and OFF clouds perpendicular to the MAD fit line, relative to the length of the combined cloud along that line.

Sub-bands in Trajectory Plots

The first ON fixation in a given scanning cycle, together with any in the contralateral (lower firing rate) half of the oculomotor range, were grouped into the first ON band (‘ON1’, gray trajectories of Fig. 9). Any ON fixations (apart from the first in the cycle) in the ipsilateral (higher firing rate) half of the oculomotor range were grouped into the second ON band (‘ON2’, black trajectories of Fig. 9). These were designed to split the ON fixations into two roughly equal sized groups, irrespective of whether a particular fish tended to use a few large saccades or many small saccades during its scanning cycle. The same analysis described above for ON versus OFF perpendicular hysteresis was performed for ON2 versus ON1 perpendicular sub-band hysteresis, using MAD fit lines to the combined ON–OFF data (above).

Results

Action potential discharge by pairs of pre-motor eye position neurons in hindbrain area I (Pastor *et al.*, 1994) was monitored while awake head-restrained goldfish performed spontaneous saccades and fixations during periods of light and dark (22 ipsilateral pairs from 14 fish). In the following, data from dark and light conditions are pooled. To achieve isolated recordings, activity from each cell in a pair was recorded using a separate electrode. Spontaneous oculomotor behavior consisted of a cyclic pattern of horizontal saccades and fixations, generally with two or more saccades towards one extreme followed by two or more saccades towards the other extreme. During this behavior, position cells on the same side of midline display steps of tonic discharge rate, with rates increasing for more ipsilateral fixations, and decreasing for more contralateral fixations (Pastor *et al.*, 1994; Aksay *et al.*, 2000).

Figure 2 shows the relationship between mean tonic firing rate and eye position during fixations for four position cells (a, b one pair, c, d second pair). To a first approximation, the firing rate of each cell increased linearly as eye position became progressively more eccentric toward the side where the cell was located. In the following, we refer to this nasal-to-temporal direction of increased firing rate as the ON direction and the opposite as the OFF direction. Note that cells can fire at low tonic rates following both ON and OFF saccades. In Figure 2 fixations following ON saccades are shown as black filled

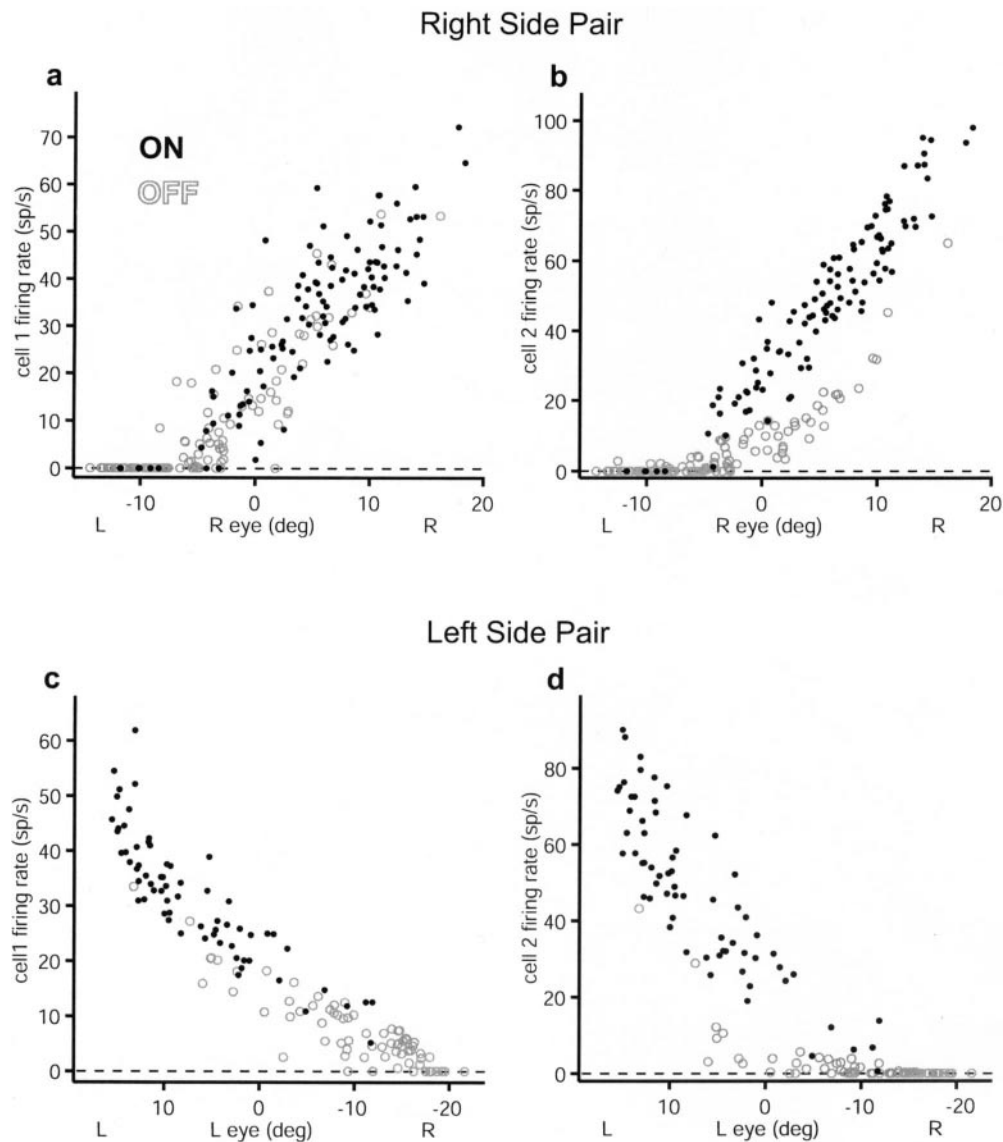


Figure 2. Relation between firing rates of position neurons in goldfish area I and eye position is generally history dependent. Tonic firing rate versus ipsilateral eye position during fixations for two pairs of cells following ON saccades (black filled circles) and OFF saccades (gray open circles). (a, b) Pair recorded from right side area I. (c, d) Pair recorded from left side area I. (Data in a and b are from pair 13 of Fig. 5. Data in c and d are from pair 6 of Fig. 5.)

circles, while those following OFF saccades are shown as gray open circles. The plot of cell a of the first pair in Figure 2 shows no systematic difference between the clouds of points from ON and OFF fixations. However, the plots from the other three cells show pronounced hysteresis between ON and OFF fixations, with the rates for a given eye position being lower during OFF fixations. In paired recordings, one cell often showed more eye-rate hysteresis than the other, although this was not quantified here. Instead, the degree of rate-rate history dependence, or pair hysteresis, was examined directly.

A basic finding is that the firing rate–firing rate relationship of many pairs was systematically different in the two directions (ON and OFF) of the scanning cycle. This pair hysteresis can be directly observed in firing rate versus time plots for a pair of neurons, as shown for two different pairs in Figure 3. The left-hand arrow indicates an ON fixation, the dashed lines indicate

for reference the average spike rate during this fixation, and the right-hand arrow indicates the first subsequent OFF fixation. For both pairs, the two cells return to their reference ON firing rates during *different* OFF fixations. For example, in Panel A, during the first OFF fixation, Cell 2 returned to about its reference firing rate. Cell 1, on the other hand, fired faster than its reference rate.

To visualize this trend over longer periods of recorded data, averaged firing rate from each fixation for one cell was plotted against the corresponding value for the other cell (Fig. 4). This is analogous to the schematic diagram in Figure 1c,d. Data were separated into two groups, those fixations following ON saccades, the ‘ON’ group, indicated by black filled circles, and those following nasally directed saccades, the ‘OFF’ group, indicated by gray open circles. Those points not lying on the axes derive from fixations where both cells were firing, with progressively ipsilateral fixations generally yielding points at

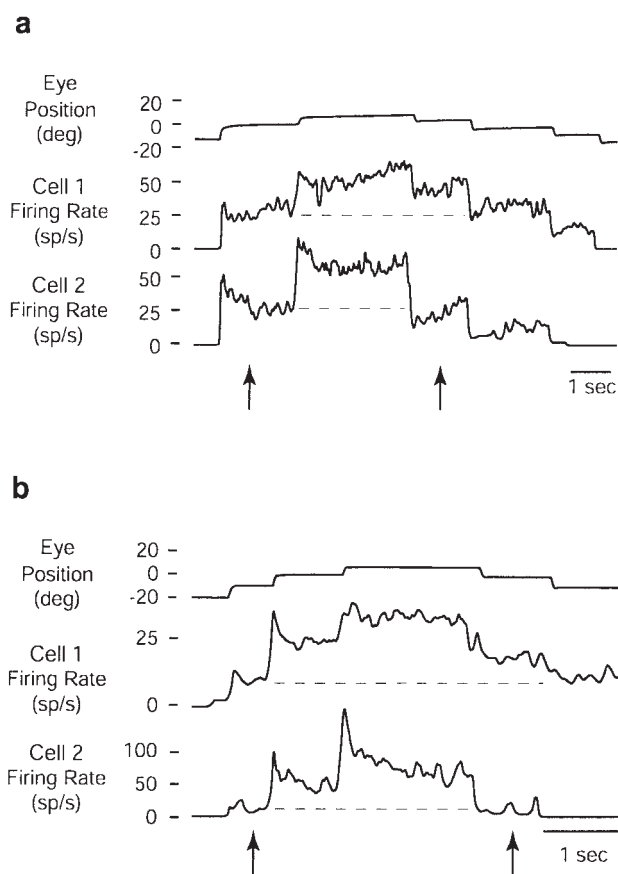


Figure 3. Relation between rates of two simultaneously recorded cells can show history dependence. (a, b) Eye position and firing rates versus time of two pairs of position cells during a sequence of saccades and fixations. Arrows indicate fixations referred to in text. Dashed line indicates average firing rate in first referenced fixation. (Data in a are from pair 13 of Fig. 5; data in b from pair 6 of Fig. 5.)

progressively higher rates. Points along the axes derive from fixations where only one cell was firing. At high firing rates, the density of ON fixations was greater than that of OFF fixations. At moderate and low rates, the density of OFF fixations increased. At moderate firing rates, when the two groups would be expected to show the most overlap, many pairs displayed separation between the cluster of points from each group. Furthermore, when the cell with the lower position threshold was plotted along the abscissa (horizontal axis), the ON cluster was generally above the OFF cluster. In other words, for a given rate of the lower threshold cell, the rate of the higher threshold cell was greater during ON fixations than during OFF fixations.

To quantify this observation, a best-fit line, in the least-squares sense, was determined from those points in the combined ON and OFF data set where both cells fired at >5 spikes/s. The cell having the largest range in firing rate was plotted along the abscissa to maximize the robustness of the fitting (Fig. 5a). The vertical deviation of each separate group (ON and OFF) from the best-fit line was measured. This calculation used only points whose abscissa value was in a region representing a firing rate from 5 to 70% of the maximum, where similar group sizes were apparent. This range is indicated by dashed vertical lines in the figure. The ON-OFF difference between the two groups in mean of the residuals, the vertical distances of the data to the best-fit line, was taken as a measure of pair hysteresis. This

procedure was repeated for the horizontal deviations. The vertical hysteresis measurements for 15 ipsilateral pairs are displayed in rank order in Figure 5b; a positive number indicates that when the low threshold neuron's rate is plotted along the abscissa, as in Figure 4, the ON cluster of fixation data points is above the OFF cluster, relative to the best fit line. For comparison, also shown are bars corresponding to the larger of the ON or OFF standard deviations of the residuals, a measure of the spread in the data. Ten out of 15 pairs had a hysteresis measure greater than their spread measure, corresponding to plots that looked clearly hysteretic by visual inspection (for example, Fig. 4a-d). For these 10, normalizing hysteresis measures by the dynamic range of the firing rate during fixations yielded a mean pair hysteresis percentage of $12.3 \pm 8.7\%$. These pairs also had a horizontal hysteresis score of the opposite sign, eliminating the possibility that the score arose simply due to the spread in the data. A *t*-test on the significance of the difference in means for these 10 pairs yielded *P*-values all less than 0.005, while a *t*-test on the remaining five pairs yielded four with *P*-values greater than 0.05 and one with *P*-value of 0.03. Restricting hysteresis measurements to the last half second of the fixation period (for those fixations at least 2 s in duration) did not appreciably alter these findings, as eight out of nine hysteretic pairs that could be evaluated remained hysteretic, with a mean hysteresis percentage of $13.3 \pm 7.9\%$ (Fig. 5c).

Cell pair hysteresis was also characterized by analysis of firing rate trajectories, allowing visualization of hysteresis throughout the fixation and a more rigorous statistical measure of significance (see Methods). To perform a trajectory analysis, firing rates during fixations were smoothed as described in the Methods section. Figure 6a shows an example of the smoothed firing rate (black) versus time of a position cell superimposed over a plot of the inverse inter-spike interval (gray). The smoothing process removes much of the high frequency noise in the firing rate while preserving the underlying slower trends. Figure 6b shows sample traces from another fish of the ipsilateral eye position and a pair of cells' smoothed firing rates against time. Each horizontal dashed black line connects an ON and an OFF fixation during which the lower threshold cell (gray) is firing at roughly the same rate. The higher threshold cell (black), by contrast, fires at a lower rate during the OFF fixation than during the corresponding ON fixation (linked arrows).

Rate versus rate trajectory plots, analogous to scatter plots for mean firing (Fig. 4), can be used to display longer periods of firing rate data. Figure 7 shows these plots (for between 2 and 10 min of data) with the smoothed rate of the lower threshold cell on the abscissa, and that of the higher threshold cell on the ordinate. Each fixation corresponds to a line of points (trajectory) in the figure. Trajectories during fixations following an ON direction saccade are black, and those following an OFF saccade are gray. Closely spaced points along a trajectory indicate periods of slowly varying rate, whereas widely spaced points along a trajectory indicate more rapid variation.

Perpendicular hysteresis scores were calculated by analyzing differences between ON and OFF data in a set of adjacent thin strips perpendicular to a minimum absolute deviation ('MAD') fit line through the combined data (see Methods and supplementary figure). A strong visual impression of hysteresis between the ON and OFF bands is evident in the trajectory plot of the cell pair in Figure 7a (pair 18 in Fig. 10, and pair 13 in Figs 3-5). Corroborating the visual impression of the trajectory plot

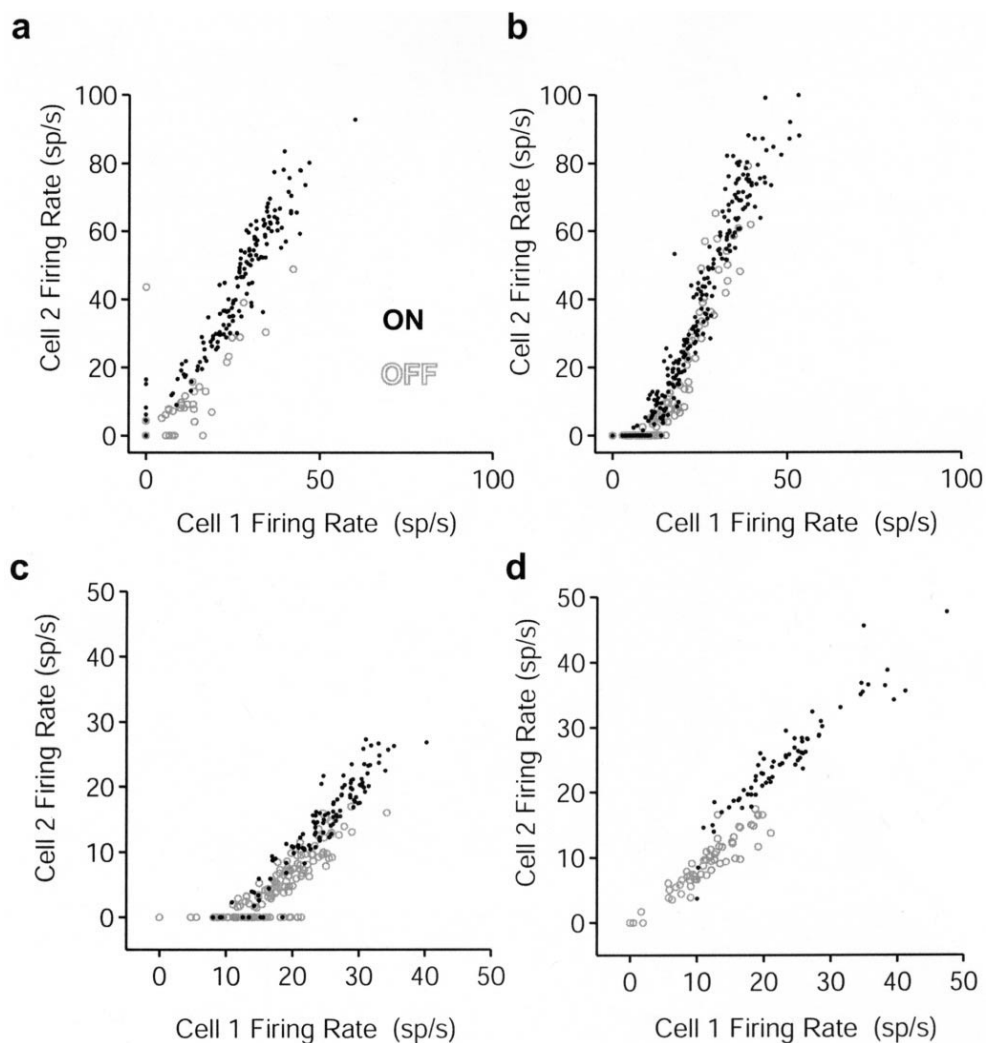


Figure 4. Scatter plots of the mean firing rate of one cell versus the mean firing rate of the second. (*a–d*) Firing rate of cell 1 versus firing rate of cell 2 during fixations following ON saccades (black filled circles) and OFF saccades (gray open circles). The firing rate of the cell with lower position threshold is oriented along the abscissa. Data in *a, b, c, d* are from pairs 13, 6, 9, 8, respectively, of Figure 5.

and the scatter-plot hysteresis, the pair had a perpendicular hysteresis score of 11.5 spikes/s for this 10 min segment of data. Overall, hysteresis scores were fairly reproducible across four consecutive 10 min periods of data, with a mean value of 6.9 spikes/s (95% confidence interval 1.7–12 spikes/s, $P = 0.02$, t -test). Panels *B* and *C* in Figure 7 show two other examples of readily apparent and statistically significant hysteresis (see legend for details), but panel 4 shows a case with no obvious pair hysteresis; the mean perpendicular hysteresis score was 0.2 spikes/s for this pair, not significantly different from zero ($P = 0.6$).

Based on trajectory plots, cell pairs were categorized as hysteretic if their mean perpendicular hysteresis scores were significantly different from zero (see Methods; the t -test used here is based on data across epochs of time). Thirteen of 21 pairs (>60%) were hysteretic by this criterion. For all 13, ON trajectories were consistently above OFF trajectories when the cell with lower eye position threshold was plotted along the abscissa.

During stable fixations, a second form of systematic non-uniqueness was apparent in the rate relationships of many

position neuron pairs. Two examples are shown in Figure 8. Here, the comparison to note is the relationship of rates during the second ON fixation of one cycle (labeled 2) to the first ON fixation of a nearby cycle (labeled 1). While the firing rate of the lower threshold cell (gray) is nearly the same for both fixations, the firing rate of the higher threshold cell (black) is higher during the ON fixations that come later in a cycle (2) than it is for fixations that come first in the cycle (1).

In order to quantify this observation, ON bands were split into two sub-bands and analyzed analogously to the ON–OFF bands. The first sub-band (ON1) included the first ON fixation in every scanning cycle, and any others following it for which the average eye position was in the contralateral half of the oculomotor range (see Methods). The second sub-band (ON2) contained all other ON fixations.

Figure 9 shows four sub-band trajectory plots (low threshold cell on abscissa). Trajectories in the ON1 band are black, those in the ON2 band are gray. Panel *a* shows the same exemplar pair as in Figure 3*a*. There is pair-hysteresis between the two sub-bands, with a perpendicular score of 11.6 spikes/s. However, across the 40 min of recorded data the mean perpendicular

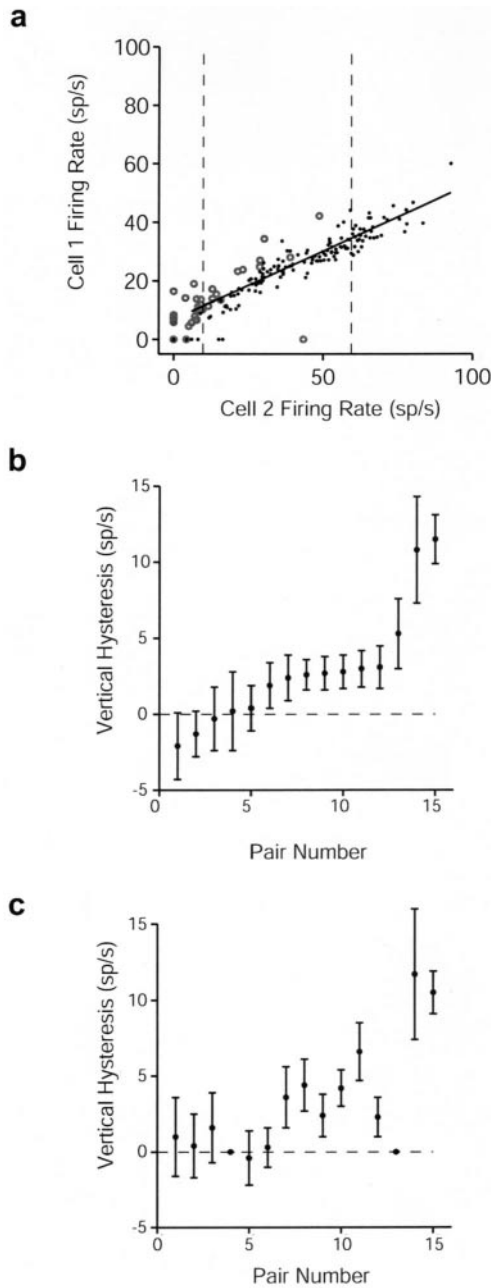


Figure 5. Assessment of pair hysteresis in scatter plots. (a) Firing rate of cell 1 versus firing rate of cell 2 during fixations following ON saccades (black filled circles) and OFF saccades (gray open circles) for pair 13. The rate of the cell with larger range of firing is oriented along the abscissa. The solid line is a regression line to data >5 spikes/s. Data between dashed lines was used for assessment of hysteresis. (b) Hysteresis scores (ON-OFF), against pair number, in order of increasing scores. (c) Hysteresis scores of the same points as in (b) when only the last 500 ms of a fixation was used. Points without error bars indicates pairs that could not be evaluated due to lack of data.

hysteresis score of 4.8 spikes/s (5.4%) was not significantly different from zero ($P = 0.14$) because of slow non-stationarities in the data.

The data in Figure 9b had a perpendicular ON2-ON1 hysteresis score of 6.7 spikes/s, with the mean across epochs for that pair being 5.1 spikes/s (10.3%, $P < 0.001$). Panel c shows another case with significant sub-band pair-hysteresis of 3.6 spikes/s

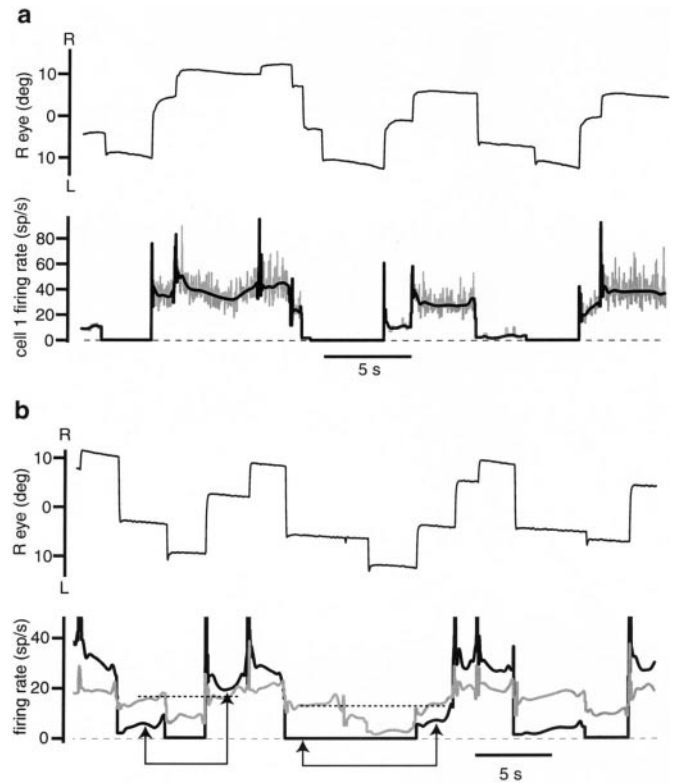


Figure 6. ON-OFF pair hysteresis in smoothed firing rates. (a) Ipsilateral eye position (top), smoothed firing rate (bottom, black) and instantaneous firing rate (bottom, gray) for a different segment of data from cell 1 in Figure 3a. (b) Ipsilateral eye position (top), smoothed firing rate of lower threshold cell (bottom, gray), and a second higher threshold cell (bottom, black) versus time. The two horizontal black dashed lines connect periods when the firing rate of the lower threshold cell was the same during an OFF fixation and the next ON fixation. Linked arrows indicate the firing rate changes of the higher threshold cell. (Data in b from pair 10 in Figure 10, recorded in the light.)

(mean 3.0 spikes/s, 5.1%, $P < 0.001$), and panel d shows a case with a small yet statistically significant amount of sub-band hysteresis (mean 1.0 spikes/s, 3.2%, $P = 0.004$).

The entire data set is summarized in Figure 10 with ON-OFF perpendicular hysteresis shown in panels a and b, and ON sub-band hysteresis in panels c and d. Pairs are ranked in order of increasing mean ON-OFF perpendicular hysteresis score, and the means and 95% confidence intervals are plotted. Significantly hysteretic pairs (confidence interval does not include zero) are indicated by asterisks (*). Twenty-one out of 22 recorded pairs had both an ON and an OFF band in which both cells were firing >2 spikes/s and could be analyzed by this procedure. Of these 21, 13 had statistically significant ON-OFF hysteresis. There were four hysteretic pairs for which the perpendicular hysteresis exceeded 5 spikes/s, three pairs for which the percentage perpendicular hysteresis score exceeded 10%, and 10 pairs for which the percentage perpendicular hysteresis score exceeded 5%. Across all pairs, the mean perpendicular ON-OFF hysteresis score was 3.1 ± 3.7 spikes/s, and the mean percentage ON-OFF score was $5.1 \pm 5.9\%$. The ON2-ON1 perpendicular sub-band hysteresis scores and confidence intervals for each pair are shown directly below the ON-OFF scores for that pair. Overall, 11 out of 22 pairs showed statistically significant sub-band hysteresis, with the mean ON2-ON1 perpendicular scores across all pairs being 2.4 ± 3.4 spikes/s and

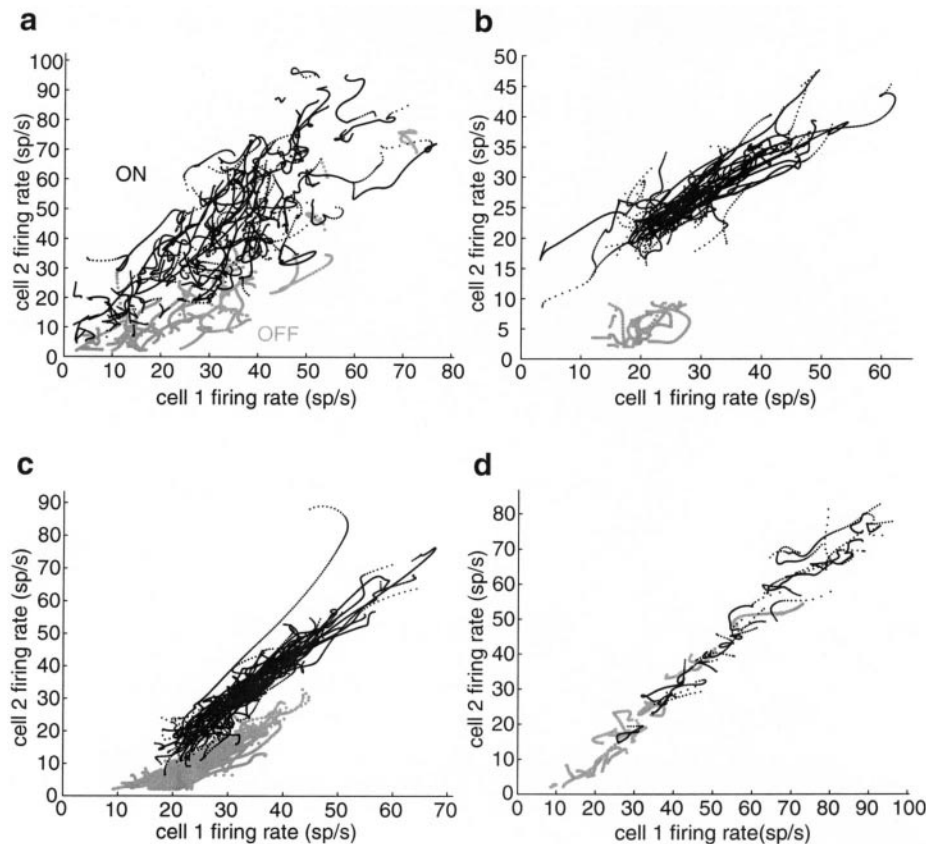


Figure 7. Trajectory plots of the smoothed firing rate of one cell versus another. (a–d) The firing rate of the lower threshold cell is oriented along the abscissa. ON fixations are indicated by smaller black points, OFF fixations are indicated by larger gray points. (a) Same pair as in Figure 3a (no. 18 in Fig. 10). Perpendicular hysteresis score (for this plot) was 11.5 spikes/s; hysteretic by our criteria. (b) Pair 21 in Figure 10. Perpendicular hysteresis score was 15.5 spikes/s; hysteretic by our criteria. (c) Pair 19 in Figure 10. Perpendicular hysteresis score was 8 spikes/s; hysteretic by our criteria. (d) Pair 4 in Figure 10. Perpendicular hysteresis score was 0 spikes/s; non-hysteretic by our criteria.

$4.0 \pm 4.5\%$. For all 11, ON2 sub-bands were consistently above ON1 sub-bands when the lower eye position threshold cell was plotted along the abscissa. When the ON–OFF and ON2–ON1 perpendicular hysteresis results are combined, 18 out of 22 pairs demonstrate at least one kind of significant hysteresis and six pairs showed both kinds.

Discussion

The results presented here were obtained by simultaneous recordings from pairs of position neurons and are the first direct measurement and analysis of rate covariation in an oculomotor integrator. Previous analyses of the rates of position neurons employed only single neuron recordings coupled with eye position measurement. As anticipated from previously observed threshold linear relationships between eye position and firing rate (Lopez-Barneo *et al.*, 1982; McFarland and Fuchs, 1992; Aksay *et al.*, 2000), rates of two neurons were, to first order, threshold linearly correlated with each other. Upon closer inspection, the relationship between rates showed substructure associated with saccade history. This history dependence was termed pair hysteresis. This was quantified for two forms. The first was termed ON–OFF hysteresis: for a given firing rate of one cell, a second cell had consistent difference between rates for ON and OFF fixations. The second was termed ON2–ON1 hysteresis: during the ON part of the scanning cycle, for a given rate of one cell, a second cell had consistently different rates

during fixations at the beginning (ON1) as compared with those nearer the end (ON2).

Patterns of Persistent Firing

A striking feature of the difference between ON and OFF rates was that the sign of the hysteresis was associated with the relative eye position thresholds of the two cells. ON–OFF hysteresis was readily apparent on ~60% of the pairs studied. On average, this hysteresis was 12.3% of the dynamic range of persistent firing. In rate–rate plots, with the lower threshold cell plotted along the abscissa, the ON fixations were generally above the OFF fixations. This trend summarizing the data is schematically illustrated in Figure 11a. A similar trend was noted previously when the relation between position neuron rate and eye position was analyzed (Aksay *et al.*, 2000): generally, firing rates were higher during ON fixations for a given eye position. Given that area I position neurons project axon collaterals to motoneurons in the abducens complex (Aksay *et al.*, 2000) and that inactivation of area I results in inability to maintain eccentric gaze (Pastor *et al.*, 1994), the ON–OFF pattern seen between rates may have a role in establishing the ON–OFF relation between eye position and rates.

The sign of the ON2–ON1 hysteresis also tended to correlate with the relative thresholds of cells. Half of the pairs studied displayed this form of hysteresis, which was on average slightly weaker than the ON–OFF hysteresis. In rate–rate plots, with the

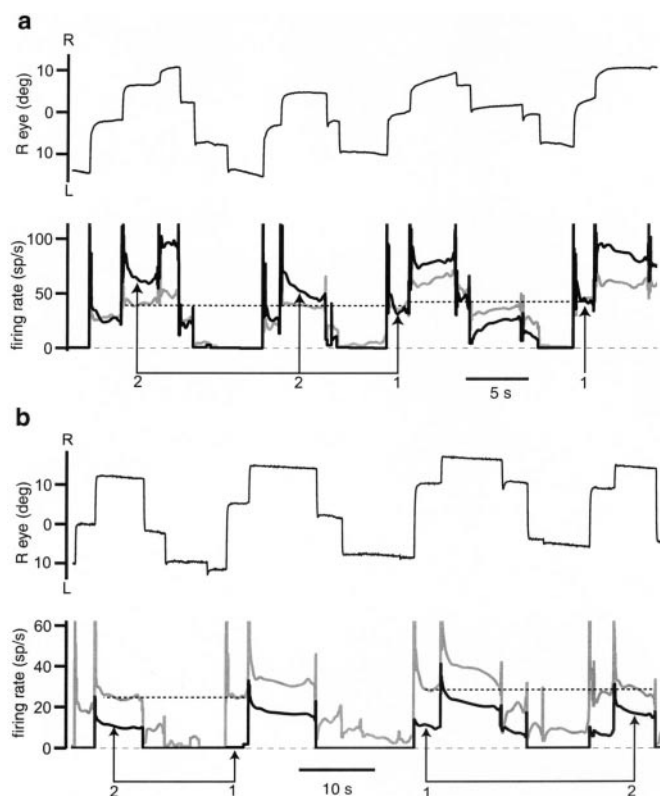


Figure 8. ON2–ON1 pair hysteresis in smoothed firing rates. Both panels: ipsilateral eye position (top sub-panel), smoothed firing rate of lower threshold cell (bottom, gray), and a higher threshold cell (bottom, black) versus time. The two horizontal black dashed lines connect periods when the firing rate of the lower threshold cell was approximately the same during an ON1 fixation (indicated by '1') and a nearby ON2 fixation (indicated by '2'). Arrows indicate the firing rate changes of the higher threshold cell. (a) Same pair as in Figures 3a and 7a (no. 18 in Fig. 10), recorded in the dark. (b) Data from pair 1 in Figure 10 (recorded with lights on).

lower threshold cell's rate plotted along the abscissa, the ON2 fixations were generally above the ON1 fixations. This trend is summarized schematically in Figure 11b. Some position neurons' tonic rates appeared to saturate at extremes of eye position (Fig. 6); if two cells had different degrees of rate saturation, this would produce a non-linear pair relationship, but not a hysteretic one. The trend in the rate–rate relationship observed here is not just a non-linearity but a non-uniqueness related to the number of preceding ON saccades.

The methods of analysis employed may underestimate the number of pairs with history dependent rate–rate covariation. First, the typical length of one analysis epoch was 10 min or more. Non-stationarity in the rate–rate relationships over many minutes may blur hysteresis as OFF fixations move into a region where there were previously only ON fixations. Second, in several cases there were too few fixations in a region of overlap between the ON and OFF bands to assess hysteresis with scatter plots. Third, an analysis of hysteresis in sub-bands of OFF fixations could not be done in many cases due to a lack of data resulting from cells falling below threshold after the second OFF fixation.

The hysteresis demonstrated may arise from differences in post-saccadic firing rate drift and/or differences in steady-state

firing rate. As visible in firing rate versus time plots in Figures 3, 6 and 8, activity of position cells during fixation was not as stable as that of eye position; there was commonly post-saccadic slow drift towards an apparent asymptotic value. Slow drifts often have history dependence, exhibiting tendency to drift downward after ON saccades and upward after OFF saccades; furthermore, they are not always equally apparent on both cells of a pair. Similar post-saccadic drift has been reported for motoneurons (Goldstein and Robinson, 1986; Fuchs *et al.*, 1988; Stahl and Simpson, 1995a; Pastor *et al.*, 1991) and pre-motor cells with eye-position sensitivity (Stahl and Simpson, 1995b). Even if asymptotic rates are linearly related to each other, presence of slow history-dependent drift on one cell and not the other (or two different decay rates) could lead to hysteretic rate–rate relationships. An attempt to distinguish between asymptotic and slow drift effects was made by comparing hysteresis over the entire fixation with hysteresis in the last half second; this revealed little systematic variation in hysteresis values, as both ON–OFF hysteresis measures were on average a little over 10% of the range. This suggests that hysteresis measurements in most cases largely reflected history dependence of asymptotic rates. However, this can only be viewed as a preliminary attempt at distinction, since post-saccadic drifts occurred on timescales comparable to the length of most fixations.

Implications for Mechanisms of Persistent Firing

The presence of hysteresis in the rate–rate relationship suggests that the pattern of persistent states encoding eye position is not constrained to a unique line. Rather, during spontaneous fixation behavior, it appears that there may be wider region of stable points, and that parts of this region are traversed in a systematic fashion through saccadic stimulation. This expanded region of stability could be generated in a number of ways: for example, through cellular or local circuit mechanisms with slow dynamics such as membrane multi-stability, and/or through multiple modes of integration in a recurrent network.

A form of cellular memory that produces action potential discharge reminiscent of activity in position neurons during a sequence of saccades and fixation has been reported in brain slice experiments with pyramidal neurons from entorhinal cortex (Egorov *et al.*, 2002). A period of strong intracellular depolarizing current injection or a tetanus of synaptic stimulation produced a prolonged membrane potential plateau and prolonged sustained discharge of action potentials, the rate of which depends upon the history of stimulation. Since this persistent activity can be sustained even in the presence of synaptic blockers, it appears that each neuron has the capacity to function as a complete integrator. If neurons in goldfish area I have such cellular multistability, the pair hysteresis observed might result from saccadic input to the two cells that differed systematically.

Intracellular recording of position neurons during scanning behavior in alert goldfish has been employed to explore if area I neurons show this form of intrinsic cellular memory (Aksay *et al.*, 2001). These experiments did not reveal bistable events when current stimulation was administered over a range of eye positions. As the recordings were primarily peri-somatic, this suggests that any putative plateau-like events would have to be located on distal dendrites.

Two recent models have explored incorporating bistable response elements within a recurrent network. In the first (Koulakov *et al.*, 2002), bistability is generated through very

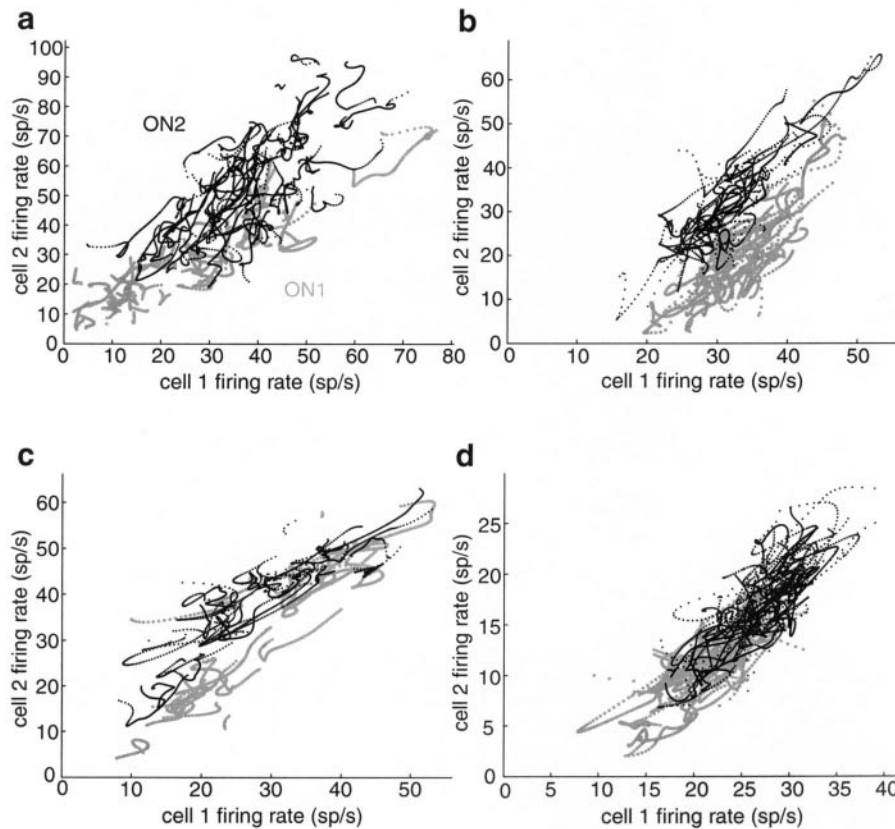


Figure 9. Trajectory plots of smoothed firing rate of one cell versus another, during ON fixations. (a–d) The firing rate of the lower threshold cell is oriented along the abscissa. ON1 fixations indicated by larger gray points and ON2 fixations by smaller black points. (a) Same pair as in Figures 3a, 7a and 8a (no. 18 in Fig. 10). ON2–ON1 perpendicular hysteresis score was 11.6 spikes/s; non-hysteretic by our criteria. (b) Pair 16 in Figure 10. ON2–ON1 perpendicular hysteresis score was 6.7 spikes/s; hysteretic by our criteria. (c) Pair 17 in Figure 10. ON2–ON1 perpendicular hysteresis score was 3.6 spikes/s; hysteretic by our criteria. (d) Pair 11 in Figure 10. ON2–ON1 perpendicular hysteresis score was 0.7 spikes/s; hysteretic by our criteria.

strong local excitatory connections [mirroring an earlier model by Rosen (1972)] or NMDA plateau potentials, and in the second (Goldman *et al.*, 2003), each cell contains multiple dendritic bistable compartments. Although not explicitly investigated, the first network apparently does generate ON–OFF rate–rate hysteresis of the form seen here (see Fig. 6 of Koulakov *et al.*, 2002). In the second model, ON–OFF hysteresis was generated by making dendritic bistability heterogeneous across the neurons, with the dendrites of higher threshold cells exhibiting bistability over a narrower range of input current (Goldman *et al.*, 2003).

In both models, it was found that an important benefit of adding bistable elements was that it made persistent activity in the recurrent network less sensitive to variations in feedback parameters like synaptic coupling; in other words, the network became more robust. Thus, hysteresis in the relationship between position neuron firing rates could be a manifestation of a solution to the fundamental problem of robustness.

An alternative explanation that does not rely on local memory elements is that a recurrent network of position cells may have two or more integrating modes. A coupled system of cells has the potential of exhibiting more than one dimension of integration, just as a coupled system of springs can display many modes of oscillation. In effect, two or more functionally independent neural integrators could co-exist within an anatomically coupled network of cells, with each cell participating to a varying degree

in each integrator (Anastasio, 1997; Seung, 2003). This class of model was first explored as a solution to the problem of any given integrating mode lacking robustness to certain perturbations (Cannon *et al.*, 1983).

Pair hysteresis could also arise from systematic differences of input to two or more anatomically co-localized but uncoupled and functionally distinct populations of integrating networks that have no feedback between them. Scenarios include separate networks for left and right eyes, or separate networks consisting either of low or high threshold neurons. Modeling efforts in this direction should take note of the evidence for position neurons in area I with two different axonal projection patterns (Aksay *et al.*, 2000).

It is also possible that hysteresis in a recurrent network could reflect eye-position related external drive that is present throughout the fixation, but that provides no net signal for the network to integrate. For example, if the strength of a balanced external drive consisting of excitatory input to some cells and inhibitory to others differed systematically as a function of the saccadic history, then pair-relationships of receiving neurons would be hysteretic. It is possible that reticular cells whose activity is related to body orientation (Aksay *et al.*, 2000) could contribute such an external drive.

It is important to note that although expanding the region of stability with features like additional modes, slow conductances or bistable dendritic elements could help explain the pair hystere-

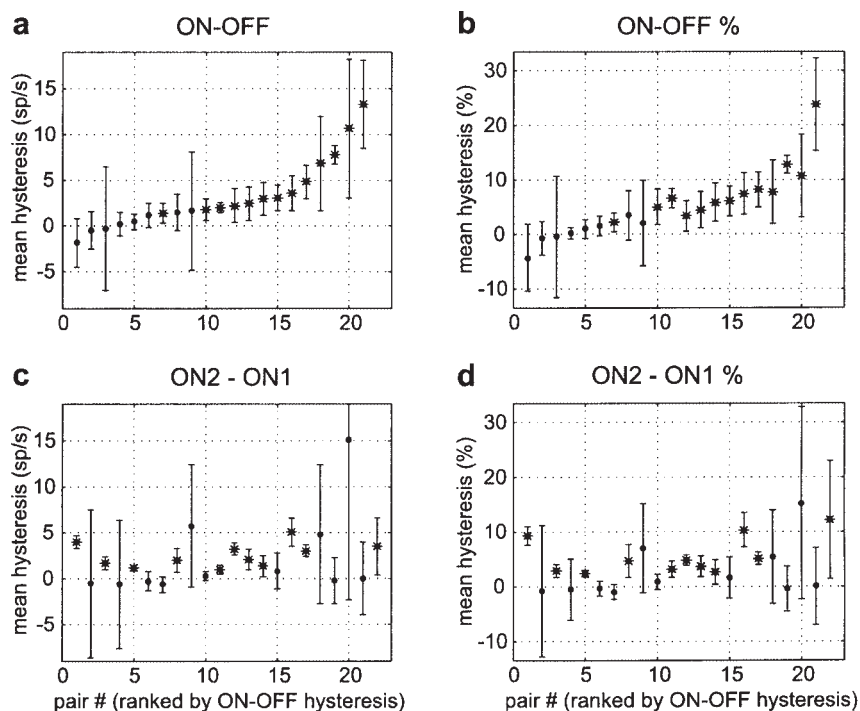


Figure 10. Summary of perpendicular pair hysteresis scores. (a–d) Pairs are plotted in rank order along the abscissa by ON–OFF hysteresis score. Mean perpendicular hysteresis scores are plotted on the ordinate, with 95% confidence intervals indicated by error bars. Points marked with asterisks indicate pairs where the scores are significantly different from zero, and are deemed hysteretic by our criteria. (a–b) ON–OFF hysteresis scores. (c–d) ON2–ON1 sub-band hysteresis scores. (a, c) Perpendicular hysteresis scores, in spikes/s. (b, d) Percentage hysteresis scores, relative to the dynamic range of firing rates along MAD fit line (see Materials and Methods).

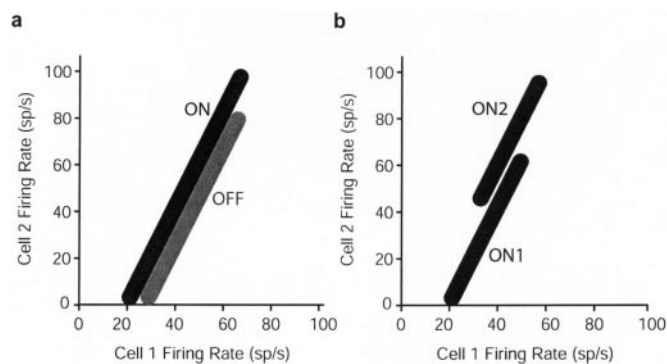


Figure 11. Summary schematic of observed hystereses. Persistent rates of lower threshold cell are represented along the abscissa, and of higher threshold cell along ordinate. (a) ON–OFF hysteresis generally results in the band of ON fixations lying above OFF fixations (gray). (b) ON2–ON1 hysteresis generally results in the band of ON2 fixations lying above the ON1 fixations.

esis and possibly generate robustness to perturbations, it can also pose a challenge if taken too far: namely, maintaining the approximately linear relation between firing rates over a wide dynamic range. Any modification to line attractor recurrent networks must retain features that have made them relevant for understanding of temporal integration in the oculomotor system. In particular, these results show that, despite hysteresis, the firing rates of the neurons must remain correlated over long periods containing tens to hundreds of fixations, with systematic deviation that has bounds, on average ~10% of the dynamic

range. In addition, the model must be capable of producing low persistent firing rates in many of the constituent neurons. Area I neurons did not demonstrate large jumps in firing rate at eye position threshold. As shown in Figures 2, 4 and 7, area I position neurons would frequently fire at tonic rates below five spikes per second during both ON and OFF fixations.

Relevance to Persistent Firing in Other Brain Areas

Questions about the importance of network mechanisms versus cellular mechanisms are very general and applicable to all systems showing persistent activity (reviewed in Durstewitz *et al.*, 2000; Wang, 2001). It is possible that the mechanisms underlying persistent neural activity generalize across brain areas and species in the same way that the basic principles of action potential generation generalize in nervous systems. Here it has been shown that in one system demonstrating persistent firing, there is not a single rigid pattern of firing for a particular memory state, but rather two or more. This systematic non-uniqueness forces a rethinking of the structure of recurrent networks in the oculomotor integrator. Hybrid models that incorporate both bistable elements and recurrent feedback may be able to generate pair hysteresis, reasonably constrained patterns of firing, and robustness to perturbation. Since recurrent networks are hypothesized mechanisms of persistent activity in other brain areas, it is important to investigate the uniqueness of ensemble persistent firing patterns in these systems.

Notes

The analyses for Figures 3–5 were carried out by E.A. The analyses for Figures 2, 6–10 and the supplementary figure were carried out by G.M.

Address correspondence to David W. Tank, Department of Molecular Biology, Princeton University, Princeton, NJ 08544, USA. Email: dwtank@princeton.edu.

Supplementary Material

Supplementary material can be found at:
<http://www.cercor.oupjournals.org/>

References

- Aksay E, Baker R, Seung HS, Tank DW (2000) Anatomy and discharge properties of pre-motor neurons in the goldfish medulla that have eye-position signals during fixations. *J Neurophysiol* 84:1035–1049.
- Aksay E, Gamkrelidze G, Seung HS, Baker R, Tank DW (2001) *In vivo* intracellular recording and perturbation of persistent activity in a neural integrator. *Nat Neurosci* 4:184–193.
- Anastasio TJ (1997) Nonuniformity of the linear network model of the oculomotor integrator produces approximately fractional-order dynamics and more realistic neuron behavior. *Biol Cybern* 79:377–391.
- Brody CD, Hernández A, Zainos A, Romo R (2003) Timing and neural encoding of somatosensory parametric working memory in macaque prefrontal cortex. *Cereb Cortex* 13:1196–1207.
- Cannon SC, Robinson DA (1985) An improved neural network for the integrator of the oculomotor system. *Biol Cybern* 53:93–108.
- Cannon SC, Robinson DA, Shamma S (1983) A proposed neural network for the integrator of the oculomotor system. *Biol Cybern* 49:127–136.
- Delgado-García JM, del Pozo F, Baker R (1986a) Behavior of neurons in the abducens nucleus of the alert cat—I. Motoneurons. *J Neurophysiol* 17:929–952.
- Delgado-García JM, del Pozo F, Baker R (1986b) Behavior of neurons in the abducens nucleus of the alert cat—II. Internuclear neurons. *Neuroscience* 17:953–973.
- Delgado-García JM, Vidal PP, Gomez C, Berthoz A (1989) A neurophysiological study of prepositus hypoglossi neurons projecting to oculomotor and preocolomotor nuclei in the alert cat. *Neuroscience* 29:291–307.
- Durstewitz D, Seamans JK, Sejnowski TJ (2000) Neurocomputational models of working memory. *Nat Neurosci* 3:1184–1191.
- Eckmiller R (1974) Hysteresis in the static characteristics of eye position coded neurons in the alert monkey. *Pflugers Arch* 350:249–258.
- Egorov AV, Hamam BN, Fransén E, Hasselmo ME, Alonso AA (2002) Graded persistent activity in entorhinal cortex neurons. *Nature* 420:133–134.
- Fuchs AF, Scudder CA, Kaneko CR (1988) Discharge patterns and recruitment order of identified motoneurons and internuclear neurons in the monkey abducens nucleus. *J Neurophysiol* 60:1874–1895.
- Fukushima K, Fukushima J, Harada C, Ohashi T, Kase M (1990) Neuronal activity related to vertical eye movement in the region of the interstitial nucleus of Cajal in alert cats. *Exp Brain Res* 79:43–64.
- Funahashi S, Bruce CJ, Goldman-Rakic PS (1989) Mnemonic coding of visual space in the monkey's dorsolateral prefrontal cortex. *J Neurophysiol* 61:331–349.
- Fuster J, Alexander G (1971) Neuron activity related to short-term memory. *Science* 173:652–654.
- Gnadt JW, Anderson RA (1988) Memory related motor planning activity in posterior parietal cortex of macaque. *Exp Brain Res* 70:216–220.
- Goldman MS, Levine JH, Major G, Tank DW, Seung HS (2003) Robust persistent neural activity in a model neural integrator with multiple hysteretic dendrites per neuron. *Cereb Cortex* 13:1185–1195.
- Goldstein HP, Robinson DA (1986) Hysteresis and slow drift in abducens unit activity. *J Neurophysiol* 55:1044–1056.
- King WM, Fuchs AF, Magnin M (1981) Vertical eye movement-related responses of neurons in midbrain near interstitial nucleus of Cajal. *J Neurophysiol* 46:549–562.
- Koulakov AA, Raghavachari S, Kepecs A, Lisman JE (2002) Model for a robust neural integrator. *Nat Neurosci* 5:775–782.
- Lopez-Barneo J, Darlot C, Berthoz A, Baker R (1982) Neuronal activity in prepositus nucleus correlated with eye movement in the alert cat. *J Neurophysiol* 47:329–352.
- Luschei ES, Fuchs AF (1972) Activity of brain stem neurons during eye movements of alert monkeys. *J Neurophysiol* 35:444–461.
- McFarland JL, Fuchs AF (1992) Discharge patterns in nucleus prepositus hypoglossi and adjacent medial vestibular nucleus during horizontal eye movement in behaving macaques. *J Neurophysiol* 68:319–332.
- Nakamura K (1999) Auditory spatial discriminatory and mnemonic neuron in rat posterior parietal cortex. *J Neurophysiol* 82:2503–2517.
- Pastor AM, Torres B, Delgado-García JM, Baker R (1991) Discharge characteristics of medial rectus and abducens motoneurons in the goldfish. *J Neurophysiol* 66:2125–2140.
- Pastor AM, de La Cruz RR, Baker R (1994) Eye position and eye velocity integrators reside in separate brainstem nuclei. *Proc Natl Acad Sci USA* 91:807–811.
- Press WH, Teukolsky SA, Vetterling WT, Flannery BP (1992) Numerical recipes in C. New York: Cambridge.
- Romanski LM, Goldman-Rakic PS (2002) An auditory domain in primate prefrontal cortex. *Nat Neurosci* 5:15–16.
- Romo R, Brody CD, Hernandez A, Lemus L (1999) Neuronal correlates of parametric working memory in the prefrontal cortex. *Nature* 399:470–473.
- Rosen MJ (1972) A theoretical neural integrator. *IEEE Trans Biomed Eng* 19:362–367.
- Seung HS (1996) How the brain keeps the eyes still. *Proc Natl Acad Sci USA* 93:13339–13344.
- Seung HS (2003) Amplification, attenuation, and integration in linear networks. In: *The handbook of brain theory and neural networks* (Arbib MA, ed.), pp. 94–97. Cambridge, MA: MIT Press.
- Seung HS, Lee DD, Reis BY, Tank DW (2000) Stability of the memory of eye position in a recurrent network of conductance-based model neurons. *Neuron* 26:259–271.
- Shen L (1989) Neural integration by short-term potentiation. *Biol Cybern* 61:319–325.
- Sklavos SK, Moschovakis AK (2002) Neural network simulations of the primate oculomotor system IV. A distributed bilateral stochastic model of the neural integrator of the vertical saccadic system. *Biol Cybern* 86:97–109.
- Stahl JS, Simpson JI (1995a) Dynamics of abducens nucleus neurons in the awake rabbit. *J Neurophysiol* 73:1383–1395.
- Stahl JS, Simpson JI (1995b) Dynamics of rabbit vestibular nucleus neurons and the influence of the flocculus. *J Neurophysiol* 73:1396–1413.
- Wang XJ (2001) Synaptic reverberation underlying mnemonic persistent activity. *Trends Neurosci* 24:455–463.